INTERNATIONAL JOURNAL FOR NUMERICAL METHODS IN FLUIDS
Int. J. Numer. Meth. Fluids **31**: 223–246 (1999)

TRANSITIONS AND INTERACTIONS OF INVISCID/VISCOUS, COMPRESSIBLE/INCOMPRESSIBLE AND LAMINAR/TURBULENT FLOWS

T.J. CHUNG[a,*]

[a] *Department of Mechanical and Aerospace Engineering, The University of Alabama in Huntsville, Huntsville, AL 35899, USA*

SUMMARY

This paper addresses the flow field-dependent variation (FDV) methods in which complex physical phenomena are taken into account in the final form of partial differential equations to be solved so that finite difference methods (FDM) or finite element methods (FEM) themselves will not dictate the physics, but rather they are no more than simply the options how to discretize between adjacent nodal points or within an element. The variation parameters introduced in the formulation are calculated from the current flow field based on changes of Mach numbers, Reynolds numbers, Peclet numbers and Damkohler numbers between adjacent nodal points, which play many significant roles, such as adjusting the governing equations (hyperbolic, parabolic and/or elliptic), resolving various physical phenomena and controlling the accuracy and stability of the numerical solution. The theory is verified by a number of example problems addressing the physical implications of the variation parameters, which resemble the flow field itself, shock capturing mechanism, transitions and interactions between inviscid/viscous, compressibility/incompressibility and laminar/turbulent flows. Copyright © 1999 John Wiley & Sons, Ltd.

KEY WORDS: flow field-dependent variation; FDM; FEM; flow interactions

1. INTRODUCTION

The inviscid/viscous interaction that may lead to compressible/incompressible and/or laminar/turbulent flows is one of the most complicated physical phenomena in fluid dynamics, thus making numerical simulations difficult. A typical example is the triple shock wave turbulent boundary layer interactions in high speed aircraft inlets, with fins and ramps. The complexity of the physics and the difficulty of numerical treatments stem from the limits, transitions and interactions between laminar and turbulent flows, compressibility and incompressibility, as well as inviscid and viscous behaviour, in which a single computational algorithm for all situations is not easily available. Transitions from one type of flows to another vary in both spatial and temporal domains and are often associated with physical instability that may subsequently cause numerical instability.

To handle both compressible and incompressible flows, attempts have been made by introducing preconditioners transforming from the conservation variables to primitive

* Correspondence to: Department of Mechanical and Aerospace Engineering, The University of Alabama in Huntsville, Huntsville, AL 35899, USA.

CCC 0271–2091/99/170223–24$17.50

variables for the solution of the Navier–Stokes system of equations [1,2]. In this process, the eigenvalues of the convection terms are well-conditioned, facilitating the solution of compressible flow at high speeds and at the same time rendering the solution of incompressible flow at low speeds simultaneously accessible. To cope with computations of the complex flow field, such as triple shock wave turbulent boundary layer interactions of double fins with a ramp mounted between them on a flat plate, a number of researchers [3–5] utilized existing numerical schemes, such as the MUSCL and TVD approaches for shock capturing [6–10] and implicit factored scheme [11] for compressible viscous flows, using the various turbulence models. Unfortunately, a mere combination of existing numerical methods developed specifically for certain aspects of the flow will not be capable of treating such overwhelmingly complex physical phenomena. Although some reasonable results of surface pressure and skin friction distributions have been reported, computations of heat transfer appear to be far from satisfactory [12].

The goal of this paper is to examine numerical schemes in which all ranges of flow speeds encompassing compressibility and incompressibility, laminar and turbulent, as well as inviscid and viscous flows are treated adequately. To this end, the flow field-dependent variation (FDV) methods have been introduced by Chung and his co-workers [13,14], in which solutions are obtained from a single algorithm dictated by the FDV parameters as calculated from the current state of flow fields. This process allows the governing equations to be modified or adjusted automatically (as to hyperbolic, parabolic or elliptic type) as called for by the current flow field in space and time. Abrupt changes of Mach number between adjacent nodal points indicate the presence of shock waves in compressible flows, whereas the rapid changes of Reynolds number represent turbulent microscale fluctuations for viscous flows. Such changes in the Peclet number are indicative of high temperature gradients. Similarly, Damkohler number changes represent finite rate chemistry or stiffness of species equations. Triple shock wave turbulent boundary layer interactions within the secondary separation regions subjected to separation shock and rear shock are characterized by simultaneous abrupt changes of Mach number, Reynolds number and Peclet number. The basic concept here is not to allow the predetermined existing computational algorithms to erroneously dictate the physics, but rather to have the computational parameters representative of the current flow field to follow and determine the true physics.

Turbulence models have been developed over the past several decades and have indeed been successful in some instances. It is conceivable that new models of turbulence may be developed in the future and they may continue to serve as important tools in CFD. Similarly, shock capturing techniques have reached the stage of great sophistication. Despite these developments, however, the performance of turbulence models and shock capturing techniques are mutually independent. When fluid particles of inviscid flow subjected to shock discontinuities come in contact with those of viscous flow subjected to microscale turbulent fluctuations, difficulties of satisfying all conservation laws of mass, momentum and energy arise. This is where inviscid/viscous, compressibility/incompressibility and laminar/turbulence interactions take place and they can not be accommodated as nature demands by a simple combination of two or more existing numerical schemes. In particular, the dilatational dissipation is difficult to resolve in high speed turbulent compressible flows. Resorting to the compressibility corrections [15,16] to the turbulent models originally designed for incompressible flows has been marginally successful. In describing the precise physics involving high temperature gradients, it is noted that the Peclet number in the energy equation may play a decisive role as much as the Reynolds number and Mach number in the momentum equations, as affected by the changes of these non-dimensional parameters between nodal points. In the secondary

boundary layer regions on both ramp and fins, the flow field continues to change in both space and time, alternating between transitions and limits of compressibility and incompressibility, laminar and turbulence as well as inviscid and viscous flows. The variation parameters in FDV, representative of turbulent microscale fluctuations as calculated from the changes of Reynolds number as well as the Mach number and Peclet number, are capable of predicting the corresponding turbulent flow field, although DNS mesh refinements are required in order to resolve Kolmogorov microscale fluctuations in high Reynolds number flows.

The FDV approach applied to the DNS mesh refinements is the most ideal choice if computational resources are available. In the mean time, if such computer resources are not available, the FDV scheme may be used in place of turbulent models with affordable mesh refinements for moderate Reynolds number flows ($Re \leq 10^5$). Thus, the purpose of the present work is to present the basic concept of FDV and demonstrate some numerical applications in simple cases with relatively coarse meshes. It is concluded that the FDV algorithm is capable of resolving transitions and interactions of inviscid/viscous, compressibility/incompressibility and laminar/turbulence for shock wave turbulent boundary layer flows.

In what follows, the FDV theory is presented in Section 2, followed by the interpretation of variation parameters in Section 3, numerical diffusion in Section 4, shock-capturing mechanism in Section 5, transitions and interactions between compressible and incompressible flows in Section 6, and transitions and interactions between laminar and turbulent flows in Section 7. Finally, some selected example problems are shown in Section 8, with conclusions and recommendations presented in Section 9.

2. FLOW FIELD-DEPENDENT VARIATION (FDV) THEORY

In general, explicit schemes may be used for high speed flows. However, if the flow field is viscous and subjected to widely disparate scales of both time and length, such as those found in turbulent flows or chemically reacting flows, then the implicit schemes must be used. In many flow situations these widely disparate scales may be confined to certain regions of the flow field making it highly desirable to have a scheme in which the level of implicitness could be varied in different locations. The most desirable scheme would be one in which variation parameters that can be automatically determined from the flow field of each location (nodal point or element) are introduced.

In the FDV theory, the traditional definitions of implicit and explicit schemes are significantly modified. Here, the variation parameters are introduced, which are calculated from the current flow field variables and serve as physical parameters dictating numerical accuracy and stability in the solution process, and most importantly allowing the transitions and interactions of different types of flows to be automatically accommodated.

The original idea of FDV methods began from the need to address the physics involved in shock wave turbulent boundary layer interactions [13,14]. In this situation, transitions and interactions of inviscid/viscous, compressible/incompressible and laminar/turbulent flows constitute not only the physical complexities but also computational difficulties. This is where the very low velocity in the vicinity of the wall ($M \cong 0$, $Re \cong 0$) and very high velocity far away from the wall ($M \cong 20$, $Re \cong 10^9$) coexist within a domain of study. Transitions from one type of flow to another and interactions between two distinctly different flows have been studied for many years both experimentally and numerically. Traditionally, incompressible flows were analysed using the pressure-based formulation with the primitive variables for the implicit solution of the Navier–Stokes system of equations together with the pressure Poisson

equation. On the other hand, compressible flows were analysed using the density-based formulation with the conservation variables for the explicit solution of the Navier–Stokes system of equations. In dealing with the domain of study that contains all speed flows with various physical properties, where the equations of state for compressible and incompressible flows are different and where the transitions between laminar and turbulent flows are involved in dilatational dissipation due to compressibility, very special and powerful numerical treatments must be provided. The FDV scheme has been devised toward resolving all of these issues.

To this end, let us consider the Navier–Stokes system of equations in conservation form,

$$\frac{\partial \mathbf{U}}{\partial t}+\frac{\partial \mathbf{F}_i}{\partial x_i}+\frac{\partial \mathbf{G}_i}{\partial x_i}=\mathbf{B}. \tag{1}$$

In expanding $\mathbf{U}^{n+1}$ in a special form of Taylor series about $\mathbf{U}^n$, we introduce the variation parameters s_1 and s_2 for the first and second derivatives of $\mathbf{U}$ with respect to time respectively,

$$\mathbf{U}^{n+1}=\mathbf{U}^n+\Delta t\frac{\partial \mathbf{U}^{n+s_1}}{\partial t}+\frac{\Delta t^2}{2}\frac{\partial^2 \mathbf{U}^{n+s_2}}{\partial t^2}+O(\Delta t^3), \tag{2}$$

where

$$\frac{\partial \mathbf{U}^{n+s_1}}{\partial t}=\frac{\partial \mathbf{U}^n}{\partial t}+s_1\frac{\partial \Delta \mathbf{U}^{n+1}}{\partial t}, \quad 0\le s_1\le 1, \tag{3a}$$

$$\frac{\partial^2 \mathbf{U}^{n+s_2}}{\partial t^2}=\frac{\partial^2 \mathbf{U}^n}{\partial t^2}+s_2\frac{\partial^2 \Delta \mathbf{U}^{n+1}}{\partial t^2}, \quad 0\le s_2\le 1, \tag{3b}$$

with $\Delta \mathbf{U}^{n+1}=\mathbf{U}^{n+1}-\mathbf{U}^n$. Substituting (3) into (2),

$$\Delta \mathbf{U}^{n+1}=\Delta t\left(\frac{\partial \mathbf{U}^n}{\partial t}+s_1\frac{\partial \Delta \mathbf{U}^{n+1}}{\partial t}\right)+\frac{\Delta t^2}{2}\left(\frac{\partial^2 \mathbf{U}^n}{\partial t^2}+s_2\frac{\partial^2 \Delta \mathbf{U}^{n+1}}{\partial t^2}\right)+O(\Delta t^3). \tag{4}$$

Notice that s_1, associated with the first time derivative, is intended to provide variations as appropriate to the convection and diffusion processes of flow field, whereas s_2, involved in the second time derivative, is to control adequate applications of artificial viscosity as required in accordance with the flow field.

In the conservation form of the Navier–Stokes system of equations, $\mathbf{F}_i$ and $\mathbf{B}$ are functions of $\mathbf{U}$, and $\mathbf{G}_i$ is a function of $\mathbf{U}$ and its gradient $\mathbf{U}_{,k}$. Thus, by the chain rule of calculus, the first and second derivative of $\mathbf{U}$ with respect to time may be written as follows:

$$\frac{\partial \mathbf{U}}{\partial t}=-\frac{\partial \mathbf{F}_i}{\partial x_i}-\frac{\partial \mathbf{G}_i}{\partial x_i}+\mathbf{B}, \tag{5a}$$

$$\frac{\partial^2 \mathbf{U}}{\partial t^2}=-\frac{\partial \mathbf{F}_i}{\partial \mathbf{U}}\frac{\partial}{\partial x_i}\left(\frac{\partial \mathbf{U}}{\partial t}\right)-\frac{\partial \mathbf{G}_i}{\partial \mathbf{U}}\frac{\partial}{\partial x_i}\left(\frac{\partial \mathbf{U}}{\partial t}\right)-\frac{\partial \mathbf{G}_i}{\partial \mathbf{U}_{,k}}\frac{\partial^2}{\partial x_i\,\partial x_k}\left(\frac{\partial \mathbf{U}}{\partial t}\right)+\frac{\partial \mathbf{B}}{\partial \mathbf{U}}\left(\frac{\partial \mathbf{U}}{\partial t}\right). \tag{5b}$$

We denote the convection Jacobian $\mathbf{a}_i$, the diffusion Jacobian $\mathbf{b}_i$, the diffusion gradient Jacobian $\mathbf{c}_{ik}$ and the source Jacobian $\mathbf{d}$ as

$$\mathbf{a}_i=\frac{\partial \mathbf{F}_i}{\partial \mathbf{U}}, \quad \mathbf{b}_i=\frac{\partial \mathbf{G}_i}{\partial \mathbf{U}}, \quad \mathbf{c}_{ik}=\frac{\partial \mathbf{G}_i}{\partial \mathbf{U}_{,k}}, \quad \mathbf{d}=\frac{\partial \mathbf{B}}{\partial \mathbf{U}}.$$

For the purpose of generality, it is assumed here that the source terms arise from additional equations for chemical species equations.

The second derivative of $\mathbf{U}$ with respect to time may now be written in terms of these Jacobians by substitution into (5b),

$$\frac{\partial^2 \mathbf{U}}{\partial t^2} = \frac{\partial}{\partial x_i}(\mathbf{a}_i + \mathbf{b}_i)\left(\frac{\partial \mathbf{F}_j}{\partial x_j} + \frac{\partial \mathbf{G}_j}{\partial x_j} - \mathbf{B}\right) + \frac{\partial^2}{\partial x_i \partial x_k}\mathbf{c}_{ik}\left(\frac{\partial \mathbf{F}_j}{\partial x_j} + \frac{\partial \mathbf{G}_j}{\partial x_j} - \mathbf{B}\right) - \mathbf{d}\left(\frac{\partial \mathbf{F}_j}{\partial x_j} + \frac{\partial \mathbf{G}_j}{\partial x_j} - \mathbf{B}\right). \tag{6}$$

Substituting (5a) and (6) into (4), and assuming the product of the diffusion gradient Jacobian with third-order spatial derivatives to be negligible, we have

$$\begin{aligned}
\Delta \mathbf{U}^{n+1} = {} & \Delta t\left[-\frac{\partial \mathbf{F}_i^n}{\partial x_i} - \frac{\partial \mathbf{G}_i^n}{\partial x_i} + \mathbf{B}^n + s_1\left(-\frac{\partial \Delta \mathbf{F}_i^{n+1}}{\partial x_i} - \frac{\partial \Delta \mathbf{G}_i^{n+1}}{\partial x_i} + \Delta \mathbf{B}^{n+1}\right)\right] \\
& + \frac{\Delta t^2}{2}\left\{\left[\frac{\partial}{\partial x_i}(\mathbf{a}_i + \mathbf{b}_i)\left(\frac{\partial \mathbf{F}_j^n}{\partial x_j} + \frac{\partial \mathbf{G}_j^n}{\partial x_j} - \mathbf{B}^n\right) - \mathbf{d}\left(\frac{\partial \mathbf{F}_i^n}{\partial x_i} + \frac{\partial \mathbf{G}_i^n}{\partial x_i} - \mathbf{B}^n\right)\right]\right. \\
& + s_2\left[\frac{\partial}{\partial x_i}(\mathbf{a}_i + \mathbf{b}_i)\left(\frac{\partial \Delta \mathbf{F}_j^{n+1}}{\partial x_j} + \frac{\partial \Delta \mathbf{G}_j^{n+1}}{\partial x_j} - \Delta \mathbf{B}^{n+1}\right)\right. \\
& \left.\left. - \mathbf{d}\left(\frac{\partial \Delta \mathbf{F}_i^{n+1}}{\partial x_i} + \frac{\partial \Delta \mathbf{G}_i^{n+1}}{\partial x_i} - \Delta \mathbf{B}^{n+1}\right)\right]\right\} + O(\Delta t^3).
\end{aligned} \tag{7}$$

The variation parameters s_1 and s_2 that appear in (7) may be accorded with appropriate physical roles by calculating them from the flow field-dependent quantities. For example, if s_1 is associated with the temporal changes (Δ terms, henceforth called fluctuations, not meant to be turbulent fluctuations) of convection, it may be calculated from the spatial changes of the Mach number between adjacent nodal points so that $s_1 = 0$ would imply no changes in convection fluctuations. Similarly, if s_1 is associated with the fluctuations of diffusion, then it may be calculated from the spatial changes of Reynolds number or Peclet number between adjacent nodal points such that $s_1 = 0$ would signify no changes in diffusion fluctuations. Therefore, the role of s_1 for diffusion is different from that of convection. Similarly, the role of s_1 for the fluctuation of the sources (such as reaction rates and heat generation) should be different from convection and diffusion. For example, we may define the fluctuation quantities associated with s_1 as

$$\begin{aligned}
& s_1\left(\frac{\partial \Delta \mathbf{F}_i^{n+1}}{\partial x_i} + \frac{\partial \Delta \mathbf{G}_i^{n+1}}{\partial x_i} - \Delta \mathbf{B}^{n+1}\right) \Rightarrow s_{1c}\frac{\partial \Delta \mathbf{F}_i^{n+1}}{\partial x_i} + s_{1d}\frac{\partial \Delta \mathbf{G}_i^{n+1}}{\partial x_i} - s_{1s}\Delta \mathbf{B}^{n+1} \\
& = \frac{\sqrt{M_{\max}^2 - M_{\min}^2}}{M_{\min}}\frac{\partial \Delta \mathbf{F}_i^{n+1}}{\partial x_i} + \frac{\sqrt{Re_{\max}^2 - Re_{\min}^2}}{Re_{\min}}\frac{\partial \Delta \mathbf{G}_i^{n+1}}{\partial x_i} - \frac{\sqrt{Da_{\max}^2 - Da_{\min}^2}}{Da_{\min}}\Delta \mathbf{B}^{n+1},
\end{aligned} \tag{8}$$

where it is seen that the variation parameter s_1 originally adopted as a single mathematical or numerical parameter has now turned into multiple physical parameters, such as the changes of Mach numbers, Reynolds numbers (or Peclet numbers) and Damkohler numbers (Da), between adjacent nodal points. The magnitudes of fluctuations of convection, diffusion and source terms are dictated by the current flow field situations in space and time. Similar assessments can be applied to the variation parameter s_2 as associated with its corresponding fluctuation terms of convection, diffusion and source. Thus, in order to provide variations to the changes of convection, diffusion and source terms differently in accordance with the current flow field situations, we reassign s_1 and s_2 associated with convection, diffusion and source terms as follows:

$$s_1\Delta\mathbf{G}_i \;\Rightarrow\; s_{1\mathrm{d}}\Delta\mathbf{G}_i = s_3\Delta\mathbf{G}_i, \qquad s_1\Delta\mathbf{B} \;\Rightarrow\; s_{1\mathrm{s}}\Delta\mathbf{B}_i = s_5\Delta\mathbf{B},$$

$$s_2\Delta\mathbf{G}_i \;\Rightarrow\; s_{2\mathrm{d}}\Delta\mathbf{G}_i = s_4\Delta\mathbf{G}_i, \qquad s_2\Delta\mathbf{B} \;\Rightarrow\; s_{2\mathrm{s}}\Delta\mathbf{B} = s_6\Delta\mathbf{B},$$

with the various variation parameters defined as

$s_{1\mathrm{c}} = s_1 =$ first-order convection variation parameter,

$s_{2\mathrm{c}} = s_2 =$ second-order convection variation parameter,

$s_{1\mathrm{d}} = s_3 =$ first-order diffusion variation parameter,

$s_{2\mathrm{d}} = s_4 =$ second-order diffusion variation parameter,

$s_{1\mathrm{s}} = s_5 =$ first-order source term variation parameter,

$s_{2\mathrm{s}} = s_6 =$ second-order source term variation parameter.

The first-order variation parameters s_1, s_3 and s_5 are flow field-dependent, whereas the second-order variation parameters s_2, s_4 and s_6 are exponentially proportional to the first-order variation parameters, and mainly act as artificial viscosity. Details of these variation parameters are given below.

2.1. Flow field-dependent variation parameters

As has been pointed out, the success of FDV methods depends on accurate calculations of flow field-dependent variation parameters. Specifically, the convection variation parameters s_1 and s_2 and diffusion variation parameters s_3 and s_4 and source term variation parameters s_5 and s_6 are dependent on Mach numbers, Reynolds numbers or Peclet numbers, and Damkohler numbers respectively. The first-order variation parameters s_1, s_3 and s_5 dictate the flow field solution accuracy, whereas the second-order variation parameters s_2, s_4 and s_6 maintain the solution stability.

2.1.1. Convection implicitness parameters.

$$s_1 = \begin{cases} \min(r, l) & r > \alpha \\ 0 & r < \alpha,\ M_{\min} \neq 0, \\ 1 & M_{\min} = 0 \end{cases} \tag{9a}$$

$$s_2 = s_1^{\eta}, \quad 0 < \eta < 1, \tag{9b}$$

with

$$r = \sqrt{M_{\max}^2 - M_{\min}^2}/M_{\min}, \tag{10}$$

where the maximum and minimum Mach numbers are calculated between the local adjacent nodal points in FDM or within an element in FEM, with α being the user-specified small number ($\alpha \cong 0.01$). The ranges of the second-order variation parameter exponent η are given in a previous paper [14]. It appears that the range in $\frac{1}{100} \leq \eta \leq \frac{1}{4}$ is adequate in most of the examples that have been reported.

2.1.2. Diffusion implicitness parameters.

$$s_3 = \begin{cases} \min(s, l) & s > \beta \\ 0 & s < \beta,\ Re_{\min} \neq 0, \quad \text{or } Pe_{\min} \neq 0\,, \\ 1 & Re_{\min} = 0, \quad \text{or } Pe_{\min} = 0 \end{cases} \tag{11a}$$

$$s_4 = s_3^{\eta}, \quad 0 < \eta < 1, \tag{11b}$$

with

$$s = \sqrt{Re_{\max}^2 - Re_{\min}^2}/Re_{\min} \quad \text{or} \quad s = \sqrt{Pe_{\max}^2 - Pe_{\max}^2}/Pe_{\min}, \tag{12a,b}$$

where the maximum and minimum Reynolds numbers or maximum and minimum Peclet numbers are calculated between the local adjacent nodal points or within an element, and β is a user-specified small number ($\beta \cong 0.01$). If temperature gradients are large it is possible that Peclet numbers instead of Reynolds numbers may dictate the diffusion variation parameters. The larger value of s_3 is to be chosen, as obtained either from (12a) or (12b).

2.1.3. Source term implicitness parameters. The source terms **B** vary in time and space when additional equations are included in (1) for chemically reacting species. For the case of chemically reacting flows, the changes in *Da* should be used.

$$s_5 = \begin{cases} \min(t, 1) & t \geq \gamma \\ 0 & t < \gamma,\ Da_{\min} \neq 0\,, \\ 1 & Da_{\min} = 0 \end{cases} \tag{13a}$$

$$s_6 = s_5^{\eta}, \quad 0 < \eta < 1, \tag{13b}$$

with

$$t = \sqrt{Da_{\min}^2 - Da_{\min}^2}/Da_{\min}, \tag{14}$$

where the maximum and minimum Damkohler numbers are calculated between the local adjacent nodal points or within an element, and γ is a user-specified small number ($\gamma \cong 0.01$).

The various definitions of Peclet number (Pe_{I}, Pe_{II}) and Damkohler number (Da_{I}, Da_{II}, Da_{III}, Da_{IV}, Da_{V}) are given in [14].

2.2. FDV equations

The final form of the FDV equations can be obtained by substituting the variation parameters, as defined in (8)–(14), into (7), leading to the residual of the form

$$\begin{aligned} \mathbf{R} = \Delta\mathbf{U}^{n+1} - \Delta t\Bigg[& -\frac{\partial \mathbf{F}_i^n}{\partial x_i} - \frac{\partial \mathbf{G}_i^n}{\partial x_i} + \mathbf{B}^n - s_1 \frac{\partial \Delta\mathbf{F}_i^{n+1}}{\partial x_i} - s_3 \frac{\partial \Delta\mathbf{G}_i^{n+1}}{\partial x_i} + s_5 \Delta\mathbf{B}^{n+1} \Bigg] \\ & - \frac{\Delta t^2}{2} \Bigg\{ \Bigg[\frac{\partial}{\partial x_i} (\mathbf{a}_i + \mathbf{b}_i) \Bigg(\frac{\partial \mathbf{F}_j^n}{\partial x_i} + \frac{\partial \mathbf{G}_j^n}{\partial x_j} - \mathbf{B}^n \Bigg) - \mathbf{d} \Bigg(\frac{\partial \mathbf{F}_i^n}{\partial x_i} + \frac{\partial \mathbf{G}_i^n}{\partial x_i} - \mathbf{B}^n \Bigg) \Bigg] \\ & + s_2 \Bigg[\frac{\partial}{\partial x_i} (\mathbf{a}_i + \mathbf{b}_i) \Bigg(\frac{\partial \Delta\mathbf{F}_j^{n+1}}{\partial x_j} \Bigg) - \mathbf{d} \frac{\partial \Delta\mathbf{F}_i^{n+1}}{\partial x_i} \Bigg] \\ & + \Bigg[\frac{\partial}{\partial x_i} (\mathbf{a}_i + \mathbf{b}_i) \Bigg(s_4 \frac{\partial \Delta\mathbf{G}_j^{n+1}}{\partial x_j} - s_6 \Delta\mathbf{B}^{n+1} \Bigg) - \mathbf{d} \Bigg(s_4 \frac{\partial \Delta\mathbf{G}_i^{n+1}}{\partial x_i} - s_6 \Delta\mathbf{B}^{n+1} \Bigg) \Bigg] \Bigg\} + O(\Delta t^3). \end{aligned} \tag{15a}$$

Now, rearranging and expressing the remaining terms associated with the variation parameters in terms of the Jacobians, we have

$$\Delta\mathbf{U}^{n+1}+\Delta t\left[s_1\left(\frac{\partial \mathbf{a}_i\Delta\mathbf{U}^{n+1}}{\partial x_i}\right)+s_3\left(\frac{\partial \mathbf{b}_i\Delta\mathbf{U}^{n+1}}{\partial x_i}+\frac{\partial^2\mathbf{c}_{ij}\Delta\mathbf{U}^{n+1}}{\partial x_i\,\partial x_j}\right)-s_5\mathbf{d}\Delta\mathbf{U}^{n+1}\right]$$
$$-\frac{\Delta t^2}{2}\left\{s_2\left[\frac{\partial^2(\mathbf{a}_i\mathbf{a}_j+\mathbf{b}_i\mathbf{a}_j)\Delta\mathbf{U}^{n+1}}{\partial x_i\,\partial x_j}-\mathbf{d}\,\frac{\partial \mathbf{a}_i\Delta\mathbf{U}^{n+1}}{\partial x_i}\right]\right.$$
$$+s_4\left[\left(\frac{\partial^2(\mathbf{a}_i\mathbf{b}_j+\mathbf{b}_i\mathbf{b}_j)\Delta\mathbf{U}^{n+1}}{\partial x_i\,\partial x_j}\right)-\mathbf{d}\left(\frac{\partial \mathbf{b}_i\Delta\mathbf{U}^{n+1}}{\partial x_i}+\frac{\partial^2\mathbf{c}_{ij}\Delta\mathbf{U}^{n+1}}{\partial x_i\,\partial x_j}\right)\right]$$
$$\left.-s_6\left[\mathbf{d}\,\frac{\partial(\mathbf{a}_i+\mathbf{b}_i)\Delta\mathbf{U}^{n+1}}{\partial x_i}-\mathbf{d}\Delta\mathbf{U}^{n+1}\right]\right\}$$
$$+\Delta t\left(\frac{\partial \mathbf{F}_i^n}{\partial x_i}+\frac{\partial \mathbf{G}_i^n}{\partial x_i}-\mathbf{B}^n\right)-\frac{\Delta t^2}{2}\left[\frac{\partial}{\partial x_i}(\mathbf{a}_i+\mathbf{b}_i)\left(\frac{\partial \mathbf{F}_j^n}{\partial x_j}+\frac{\partial \mathbf{G}_j^n}{\partial x_j}-\mathbf{B}^n\right)-\mathbf{d}\left(\frac{\partial \mathbf{F}_i^n}{\partial x_i}+\frac{\partial \mathbf{G}_i^n}{\partial x_i}-\mathbf{B}^n\right)\right]$$
$$+O(\Delta t^3)=0, \tag{15b}$$

with

$$\Delta\mathbf{B}^{n+1}=\frac{\partial \mathbf{B}}{\partial \mathbf{U}}\Delta\mathbf{U}^{n+1}=\mathbf{d}\Delta\mathbf{U}^{n+1}.$$

Here, once again, the product of the diffusion gradient Jacobian with third-order spatial derivatives is neglected and all Jacobians $\mathbf{a}_i$, $\mathbf{b}_i$, $\mathbf{c}_{ij}$ and $\mathbf{d}$ are assumed to remain constant spatially within each time step and to be updated at subsequent time steps. For simplicity, we may rearrange (15b) in a compact form as

$$\mathbf{R}=\mathbf{A}\Delta\mathbf{U}^{n+1}+\frac{\partial}{\partial x_i}(\mathbf{E}_i\Delta\mathbf{U}^{n+1})+\frac{\partial^2}{\partial x_i\,\partial x_j}(\mathbf{E}_{ij}\Delta\mathbf{U}^{n+1})+\mathbf{Q}^n+O(\Delta t^3), \tag{15c}$$

or

$$\left(\mathbf{A}+\frac{\partial}{\partial x_i}\mathbf{E}_i+\frac{\partial^2}{\partial x_i\,\partial x_j}\mathbf{E}_{ij}\right)\Delta\mathbf{U}^{n+1}=-\mathbf{Q}^n, \tag{16}$$

with

$$\mathbf{A}=\mathbf{I}-\Delta t s_5\mathbf{d}-\frac{\Delta t^2}{2}s_6\mathbf{d}, \tag{17a}$$

$$\mathbf{E}_i=\Delta t(s_1\mathbf{a}_i+s_3\mathbf{b}_i)+\frac{\Delta t^2}{2}[s_6\mathbf{d}(\mathbf{a}_i+\mathbf{b}_i)+s_2\mathbf{d}\mathbf{a}_i+s_4\mathbf{d}\mathbf{b}_i], \tag{17b}$$

$$\mathbf{E}_{ij}=\Delta t s_3\mathbf{c}_{ij}-\frac{\Delta t^2}{2}[s_2(\mathbf{a}_i\mathbf{a}_j+\mathbf{b}_i\mathbf{a}_j)+s_4(\mathbf{a}_i\mathbf{b}_j+\mathbf{b}_i\mathbf{b}_j-\mathbf{d}\mathbf{c}_{ij})], \tag{17c}$$

$$\mathbf{Q}^n=\frac{\partial}{\partial x_i}\left[\left(\Delta t+\frac{\Delta t^2}{2}\mathbf{d}\right)(\mathbf{F}_i^n+\mathbf{G}_i^n)+\frac{\Delta t^2}{2}(\mathbf{a}_i+\mathbf{b}_i)\mathbf{B}^n\right]-\frac{\partial^2}{\partial x_i\,\partial x_j}\left[\frac{\Delta t^2}{2}(\mathbf{a}_i+\mathbf{b}_i)(\mathbf{F}_j^n+\mathbf{G}_j^n)\right]$$
$$-\left(\Delta t+\frac{\Delta t^2}{2}\mathbf{d}\right)\mathbf{B}^n. \tag{17d}$$

An alternative scheme is to allow the source term in the left-hand-side of (16) to lag from $n+1$ to n so that (16) may be written as

$$\left(\mathbf{I}+\frac{\partial}{\partial x_i}\mathbf{E}_i+\frac{\partial^2}{\partial x_i\,\partial x_j}\mathbf{E}_{ij}\right)\Delta\mathbf{U}^{n+1}=-\mathbf{Q}^n, \tag{18}$$

$$\mathbf{Q}^n=\frac{\partial}{\partial x_i}\left[\left(\Delta t+\frac{\Delta t^2}{2}\mathbf{d}\right)(\mathbf{F}_i^n+\mathbf{G}_i^n)+\frac{\Delta t^2}{2}(\mathbf{a}_i+\mathbf{b}_i)\mathbf{B}^n\right]-\frac{\partial^2}{\partial x_i\,\partial x_j}\left[\frac{\Delta t^2}{2}(\mathbf{a}_i+\mathbf{b}_i)(\mathbf{F}_j^n+\mathbf{G}_j^n)\right]$$
$$-\left(\Delta t s_5+\frac{\Delta t^2}{2}s_6\right)\mathbf{d}\Delta\mathbf{U}^n-\left(\Delta t+\frac{\Delta t^2}{2}\mathbf{d}\right)\mathbf{B}^n. \tag{19}$$

Note that the Beam–Warming scheme [11] can be written in the form similar to (18) with the following definitions of $\mathbf{E}_i$, $\mathbf{E}_{ij}$ and $\mathbf{Q}^n$

$$\mathbf{E}_i=m\Delta t(\mathbf{a}_i+\mathbf{b}_i),\quad \text{with } m=\theta/(1+\xi), \tag{20a}$$

$$\mathbf{E}_{ij}=m\Delta t\,\mathbf{c}_{ij}, \tag{20b}$$

$$\mathbf{Q}^n=\frac{\Delta t}{1+\xi}\left(\frac{\partial\mathbf{F}_i^n}{\partial x_i}+\frac{\partial\mathbf{G}_i^n}{\partial x_i}\right)+\frac{\xi}{1+\xi}\Delta\mathbf{U}^n, \tag{20c}$$

where the cross-derivative terms appearing in $\mathbf{Q}^n$ for the Beam–Warming scheme are included in the second derivative terms on the left-hand-side. The Beam–Warming scheme is seen to be a special case of the FDV equations if we set $s_1=s_3=m$, $s_2=s_4=s_5=s_6=0$, in (18), with adjustments of $\mathbf{Q}^n$ on the right-hand-side, as in (20c). The stability analysis of the Beam–Warming scheme requires $\xi\geq 0.385$ and $\theta=\frac{1}{2}+\xi$. This will fix the variation parameter m to be $0.639\leq m\leq 0.75$. Either FDM, FEM or FVM approximations can be applied to (16) or (18). It can be shown that the FDV equations as derived in (16) and (18) are capable of producing many existing FDM and FEM schemes as special cases. We discuss these topics in Section 4 for FEM and Section 5 for FDM.

3. INTERPRETATION OF VARIATION PARAMETERS ASSOCIATED WITH JACOBIANS

The flow field-dependent variation parameters as defined earlier are capable of allowing various numerical schemes to be automatically generated. They are summarized as follows:

(a) **First-order variation parameters**. The first-order variation parameters s_1 and s_3 control all high-gradient phenomena, such as shock waves and turbulence. These parameters as calculated from the changes of local Mach numbers and Reynolds (or Peclet) numbers within each element and are indicative of the actual local element flow fields. The contours of these parameters closely resemble the flow fields themselves, with both s_1 and s_3 being large (close to unity) in regions of high gradients, but small (close to zero) in regions where the gradients are small. See Example (1) and Figure 1 for this demonstration. The basic role of s_1 and s_3 is to provide computational accuracy.

(b) **Second-order variation parameters**. The second-order variation parameters s_2 and s_4 are also flow field-dependent, exponentially proportional to the first-order variation parameters. However, their primary role is to provide adequate computational stability (artificial viscosity) as they were originally introduced into the second-order time derivative term of the Taylor series expansion of the conservation flow variables $\mathbf{U}^{n+1}$.

(c) **Elliptic/parabolic equations**. The s_1 terms represent convection. This implies that if $s\cong 0$ then the effect of convection is small. The computational scheme is automatically altered to take this effect into account, with the governing equations being predominantly parabolic–elliptic.

(d) **Hyperbolic equations**. The s_3 terms are associated with diffusion. Thus, with $s_3 \cong 0$, the effect of viscosity or diffusion is small and the computational scheme is automatically switched to that of Euler equations where the governing equations are predominantly hyperbolic.

(e) **Mixed equations**. If the first-order variation parameters s_1 and s_3 are non-zero, this indicates a typical situation for the mixed hyperbolic, parabolic and elliptic nature of the Navier–Stokes system of equations, with convection and diffusion being equally important. This is the case for incompressible flows at low speeds. The unique property of the FDV scheme is its capability to control pressure oscillations adequately without resorting to the separate hyperbolic–elliptic pressure equation for pressure corrections. The capability of FDV scheme to handle incompressible flows is achieved by a delicate balance between s_1 and s_3 as determined by the local Mach numbers and Reynolds (or Peclet) numbers. If the flow is completely incompressible ($M = 0$), the criteria given by (9) leads to $s_1 = 1$, whereas the variation parameter s_3 is to be determined according to the criteria given in (11). Make a note of the presence of the convection–diffusion interaction terms given by the product of $\mathbf{b}_i\mathbf{a}_j$ in the s_2 terms and $\mathbf{a}_i\mathbf{b}_j$ in the s_4 terms. These terms allow interactions between convection and diffusion in the viscous incompressible and/or viscous compressible flows.

(f) **High temperature gradients**. If temperature gradients rather than velocity gradients dominate the flow field, then s_3 is governed by the Peclet number rather than by the Reynolds number. Such cases arise in high-speed, high-temperature compressible flows close to the wall.

(g) **Finite rate chemistry**. In the case of reacting flows, the source term **B** contains the reaction rates that are functions of the flow field variables. With widely disparate time and length scales involved in the fast and slow chemical reaction rates of various chemical species as characterized by Damkohler numbers, the first-order source term variation parameter s_5 is instrumental in dealing with the stiffness of the resulting equations to obtain convergence to accurate solutions. On the other hand, the second-order source term variation parameter s_6 contribute to the stability of solutions. It is seen that the criteria given by Equations (13) and (14) will adjust the reaction rate terms in accordance with the ratio of the diffusion time to the reaction time in finite rate chemistry so as to assure the accurate solutions with computational stability.

(h) **Laminar/turbulent flows**. The transition to turbulence is a natural flow process as the Reynolds number increases, causing the gradients of any or all flow variables to increase. This phenomenon is the physical instability and is detected by the increase of s_3 if the flow is incompressible, but by both s_3 and s_1 if the flow is compressible. Such physical instability is likely to trigger the numerical instability, but will be countered by the second-order variation parameters s_2 and/or s_4 to ensure numerical stability automatically. In this process, these flow field dependent variation parameters are capable of capturing relaminarization, compressibility effect or dilatational turbulent energy dissipation, and turbulent unsteady fluctuations.

(i) **Error indicators**. An important contribution of the first-order variation parameters is the fact that they can be used as error indicators for adaptive mesh generations. That is, the larger the implicitness parameters, the higher the gradients of any flow variables. Whichever governs (largest first-order variation parameters) will indicate the need for mesh refinements. In this case, all variables (density, velocity, pressure, temperature, species mass fraction) participate in resolving the adaptive mesh, contrary to the conventional definitions of the error indicators.

(j) **Variation parameters/Jacobians**. Physically, the variation parameters will influence the magnitudes of Jacobians. Two different definitions of Peclet number (Pe_{I}, Pe_{II}) would require the s_3 and s_4 as calculated from the energy and species equations to be applied to the corresponding terms of the Jacobians. Similar applications for the source term variation parameters s_5 and s_6 should be followed for the source term Jacobian **d**, based on the various

definitions of Damkohler number (Da_{I}, Da_{II}, Da_{III}, Da_{IV}, Da_{V}). In this way, high-temperature gradients arising from the momentum and energy equations and the finite rate chemistry governed by the energy and species equations can be resolved accordingly.

4. NUMERICAL DIFFUSION

Note that the numerical diffusion is implicitly embedded in the FDV equations. This can be demonstrated by writing (15a) separately for the equations of momentum, continuity and energy. Combining the momentum and continuity equations and reconstructing the original differential equations, we identify the numerical diffusion terms that are produced for all governing equations as a consequence of FDV formulations. We summarize the reconstructed equations of momentum, continuity and energy without the source terms as follows: from (15a), the momentum equation is written in the form

$$\begin{aligned}\Delta(\rho v_j)^{n+1} = {} & \Delta t[-(\rho v_i v_j)_{,i} - p_{,j} + \tau_{ij_{,i}}]^n - \Delta t[s_1(\Delta(\rho v_i v_j)_{,i} + \Delta p_{,j}) - s_3 \Delta \tau_{ij_{,i}}]^{n+1} \\ & + \frac{\Delta t^2}{2}[(a_k^{(m)} + b_k^{(m)})((\rho v_i v_j)_{,i} + p_{,j} - \tau_{ij_{,i}})]^n_{,k} \\ & + \frac{\Delta t^2}{2}[(a_k^{(m)} + b_k^{(m)})(s_2(\Delta(\rho v_i v_j)_{,i} + p_{,j}) - s_4 \Delta \tau_{ij_{,i}})]^{n+1}_{,k}, \end{aligned} \tag{21}$$

where $a_k^{(m)}$ and $b_k^{(m)}$ denote the convection and diffusion Jacobians respectively for the momentum equations. Rearranging (21) to reconstruct the differential equations of momentum, we obtain

$$\frac{\partial}{\partial t}(\rho v_j) + (\rho v_i v_j + p\delta_{ij} - \tau_{ij})_{,i} = S_j(m), \tag{22}$$

with

$$\begin{aligned} S_j(m) = {} & -[s_1(\Delta \rho v_i v_j + p\delta_{ij}) - s_3 \Delta \tau_{ij}]_{,i} + \frac{\Delta t}{2}[(a_k^{(m)} + b_k^{(m)})((\rho v_i v_j)_{,i} + p_{,j} - \tau_{ij_{,i}})]_{,k} \\ & + \frac{\Delta t}{2}[(a_k^{(m)} + b_k^{(m)})(s_2(\Delta(\rho v_i v_j)_{,i} + \Delta p_{,j}) - s_4 \Delta \tau_{ij_{,i}})]_{,k}. \end{aligned} \tag{23}$$

Similarly, the FDV equation for continuity from (15a) becomes

$$\Delta \rho^{n+1} = \Delta t[-(\rho v_i)^n_{,i} - s_1 \Delta(\rho v_j)^{n+1}_{,j}] + \frac{\Delta t^2}{2}[(a_i^{(c)}(\rho v_j)_{,j})_{,i} + s_2(a_i^{(c)} \Delta(\rho v_j)_{,j})_{,i}]^{n+1}, \tag{24}$$

with $a_i^{(c)}$ being the convection Jacobian for the continuity equation. Substituting (21) into (24) and reconstructing the differential equation of continuity,

$$\frac{\partial \rho}{\partial t} + (\rho v_i)_{,i} = S(c), \tag{25}$$

with

$$\begin{aligned} S(c) = {} & \Delta t s_1[(\rho v_i v_j)_{,i} + p_{,j} - \tau_{ij_{,i}}]_{,j} - \Delta t s_1[s_1(\Delta(\rho v_i v_j)_{,i} + \Delta p_{,j}) - s_3 \Delta g t_{ij_{,i}}]_{,j} \\ & - \frac{\Delta t^2}{2} s_1[(a_k^{(m)} + b_k^{(m)})((\rho v_i v_j)_{,i} + p_{,j} - \tau_{ij_{,i}})]_{,kj} \\ & - \frac{\Delta t^2}{2} s_1[(a_k^{(m)} + b_k^{(m)})(s_2(\Delta(\rho v_i v_j)_{,i} + \Delta p_{,j}) - s_4 \Delta \tau_{ij_{,i}})]_{,kj} + \frac{\Delta t}{2}(a_i^{(c)}(\rho v_j)_{,j})_{,i}, \end{aligned} \tag{26}$$

where the third derivative associated with s_2 is neglected. A glance at (22) and (25) reveals that the right-hand-side terms $S(m)$ for momentum and $S(c)$ for continuity are the additional terms of higher-order derivatives arising from the process of derivations of the FDV equations.

The FDV equation for energy is of the form

$$\begin{aligned}\Delta(\rho E)^{n+1} = {} & \Delta t[-(\rho E v_i + p v_i)_{,i} + (\tau_{ij} v_j)_{,i} + k T_{,ii}]^n \\ & - \Delta t\{s_1[\Delta(\rho E v_i) + p v_i]_{,i} - s_3[\Delta(\tau_{ij} v_j) + k T_{,i}]_{,i}\}^{n+1} \\ & + \frac{\Delta t^2}{2}\{(a_k^{(e)} + b_k^{e})[(\rho E v_i + p v_i)_{,i} - (\tau_{ij} v_j)_{,i} - k T_{,ii}]\}_{,k}^{n} \\ & + \frac{\Delta t^2}{2}\{(a_k^{(e)} + b_k^{(e)})[s_2 \Delta(\rho E v_i + p v_i)_{,i} - s_4 \Delta(\tau_{ij} v_j + k T_{,i})_{,i}]\}_{,k}^{n+1}, \end{aligned} \tag{27}$$

which leads to the reconstructed equation of energy,

$$\frac{\partial(\rho E)}{\partial t} + [-(\rho E v_i + p v_i)_{,i} + (\tau_{ij} v_j)_{,i} + k T_{,ii}] = S(e), \tag{28}$$

with

$$\begin{aligned} S(e) = {} & \{s_1[\Delta(\rho E v_i) + p v_i]_{,i} - s_3[\Delta(\tau_{ij} v_j) + k T_{,i}]_{,i}\} \\ & + \frac{\Delta t}{2}\{(a_k^{(e)} + b_k^{(e)})[(\rho E v_i + p v_i) - (\tau_{ij} v_j)_{,i} - k T_{,ii}]\}_{,k} \\ & + \frac{\Delta t}{2}\{(a_k^{(e)} + b_k^{(e)})[s_2 \Delta(\rho E v_i + p v_i)_{,i} - s_4 \Delta(\tau_{ij} v_j + k T_{,i})_{,i}]\}_{,k}. \end{aligned} \tag{29}$$

It is interesting to note that if we neglect all incremental (fluctuation) terms, we arrive at the results identical or analogous to many of the recent developments in FEM for the treatment of convection dominated flows [17–21], including the generalized Petrov–Galerkin (GPG) methods, characteristic Galerkin methods (CGM), streamline upwind Petrov–Galerkin (SUPG) methods, space–time Galerkin/least-squares (GLS) methods, and subgrade scale (SGS) methods. To demonstrate this analogy, let us neglect all incremental and higher-order terms, but retain only the second-order derivative terms, with $s_1 = \frac{1}{2}$, so that we may arrive at the form more easily recognizable. Here, all components of convection and diffusion Jacobians can be shown to be the velocity components, $a_i^{(m)} = a_i^{(c)} = a_i^{(e)} = v_i$. These arrangements lead to

Momentum

$$\frac{\partial}{\partial t}(\rho v_j) + (\rho v_i v_j)_{,i} + p_{,j} - \tau_{ij,i} = S_j(m), \tag{30}$$

with

$$S_j(m) = \frac{\Delta t}{2}[v_k(\rho v_i v_j + p\delta_{ij} - \tau_{ij})_{,i}]_{,k}. \tag{31}$$

Continuity

$$\frac{\partial \rho}{\partial t} + (\rho v_i)_{,i} = S(c), \tag{32}$$

with

$$S(c) = \frac{\Delta t}{2}[(\rho v_i v_j)_{,ij} + p_{,jj} - \tau_{ij,ij} + (v_i(\rho v_j)_{,j})_{,i}]. \tag{33}$$

Energy

$$\frac{\partial}{\partial t}(\rho E) + [(\rho E + p)v_i - kT_{,i} - \tau_{ij}v_j]_{,i} = S(e), \tag{34}$$

with

$$S(e) = \frac{\Delta t}{2}\{v_k[((\rho E + p)v_i)_{,i} - kT_{,ii} - (\tau_{ij}v_j)_{,i}]\}_{,k} \tag{35}$$

Examining the right-hand-side terms for all equations, they are identified as numerical diffusion that arise from GPG or CGM formulations. It is seen that second derivatives of pressure arise on right-hand-side explicitly.

Returning to the FDV equations, it is important to realize that the significant contributions of FDV reside in the fluctuation terms associated with the variation parameters in (23), (26) and (29), which contribute to accuracy as well as stability of the solution process, far beyond what the currently available numerical schemes may provide. With all incremental and higher-order terms associated with variation parameters retained, we may use the fractional step procedures to solve (22), (25) and (28), using FDM, FEM or FVM. Although the fractional step solutions are equivalent to the simultaneous solutions of (16) or (18), the example problems presented in Section 3 are based on the simultaneous solutions of (16) using FEM.

In the following sections, we discuss the special features available in FDV, including the shock-capturing mechanism, transitions and interactions between compressibility and incompressibility, and transitions and interactions between laminar and turbulent flows.

5. SHOCK-CAPTURING MECHANISM

The shock-capturing mechanism is built into the FDV equations of momentum, continuity and energy. For example, let us examine (7), (15) or (21), or more specifically, the contribution from the right-hand-side terms of the momentum equation (21) by excluding the s_3 and s_4 terms.

$$\begin{aligned}
&\Delta(\rho v_j)^{n+1} + \Delta t[(\rho v_i v_j)_{,i} p_{,j} - \tau_{ij,i}]^n \\
&= -s_1 \Delta t(\Delta \rho v_i v_j + \Delta p \delta_{ij})^{n+1}_{,i} + s_2 \frac{\Delta t^2}{2}(a_k^{(m)} + b_k^{(m)})[\Delta(\rho v_i v_j)_{,i} + \Delta p_{,j}]^{n+1}_{,k} \\
&\quad + \frac{\Delta t^2}{2}(a_k^{(m)} + b_k^{(m)})[(\rho v_i v_j)_{,i} + p_{,j}]^n_{,k} \\
&= -\frac{\sqrt{M_{\max}^2 - M_{\min}^2}}{M_{\min}}(*)^{n+1} + \frac{\Delta t}{2}\left(\frac{\sqrt{M_{\max}^2 - M_{\min}^2}}{M_{\min}}\right)^{\eta}(**)^{n+1} + \frac{\Delta t}{2}(***)^n.
\end{aligned} \tag{36}$$

To identify the shock-capturing mechanism in the FDV formulation as compared with the TVD finite difference scheme, let us rewrite (36) for the one-dimensional momentum equation, retaining only the convection flux

$$\Delta u^{n+1} = -\Delta t s_1 \frac{\partial a \Delta u^{n+1}}{\partial x} + \frac{\Delta t^2}{2} s_2 a^2 \frac{\partial^2 \Delta u^{n+1}}{\partial x^2} - \Delta t \frac{\partial f^n}{\partial x} + \frac{\Delta t^2}{2} a \frac{\partial^2 f^n}{\partial x^2} \tag{37}$$

or

$$\Delta u^{n+1} = -\Delta t \frac{\sqrt{M_{\max}^2 - M_{\min}^2}}{M_{\min}} \frac{\partial a \Delta u^{n+1}}{\partial x} + \frac{\Delta t^2}{2} \left(\frac{\sqrt{M_{\max}^2 - M_{\min}^2}}{M_{\min}} \right)^{\eta} a^2 \frac{\partial^2 \Delta u^{n+1}}{\partial x^2} - \Delta t \frac{\partial f^n}{\partial x} + \frac{\Delta t^2}{2} a \frac{\partial^2 f^n}{\partial x^2},$$

where f is the convection flux and a is the one-dimensional convection Jacobian or speed of sound. The FDM analogue of (37) at node i becomes

$$\frac{\Delta u_i^{n+1}}{\Delta t} = -s_1 a \frac{1}{\Delta x} (\Delta u_i^{n+1} - \Delta u_{i-1}^{n+1}) + s_2 a^2 \Delta t \frac{1}{2\Delta x^2} (\Delta u_i^{n+1} - 2\Delta u_{i-1}^{n+1} + \Delta u_{i-2}^{n+1}) - \frac{1}{\Delta x} (f_i^n - f_{i-1}^n) + a\Delta t \frac{1}{2\Delta x^2} (f_i^n - 2f_{i-1}^n + f_{i-2}^n). \tag{38}$$

The second-order TVD semi-discretized scheme with limiter functions [6–10] is written at node i as

$$\frac{\mathrm{d}u_i}{\mathrm{d}t} = -\frac{a^+}{\Delta x} \left[1 + \Psi_{i-1/2}^+ - \frac{1}{2} \frac{\Psi_{i-3/2}^+}{r_{1-3/2}^+} \right] (u_i - u_{i-1}) - \frac{a^-}{\Delta x} \left[1 + \Psi_{i+1/2}^- - \frac{1}{2} \frac{\Psi_{i+3/2}^-}{r_{i+3/2}^-} \right] (u_{i+1} - u_i), \tag{39}$$

where Ψ and r denote the limiter function and velocity ratio respectively,

$$r_{i-3/2}^+ = \frac{u_i - u_{i-1}}{u_{i-1} - u_{i-2}}, \qquad r_{i+3/2}^- = \frac{u_{i+1} - u_{i-1}}{u_{i+2} - u_{i+1}}. \tag{40}$$

Inserting (40) into (39) yields

$$\frac{\mathrm{d}u_i}{\mathrm{d}t} = -\frac{a^+}{\Delta x} \left[(u_i - u_{i-1}) + \frac{1}{2} \Psi_{i-1/2}^+ (u_i - u_{i-1}) + \Psi_{i-3/2}^+ (u_{i-1} - u_{i-2}) \right] - \frac{a^-}{\Delta x} \left[(u_{i+1} - u_i) + \frac{1}{2} \Psi_{i+1/2}^- (u_{i+1} - u_i) - \Psi_{i+3/2}^- (u_{i+2} - u_{i-1}) \right]. \tag{41a}$$

Let us assume that

$$u_i = u_i^n + s\Delta u_i^{n+1}, \quad a^- = 0, \quad a^+ = a, \quad \Psi_{i-1/2}^+ = 2\Psi_{i-3/2}^+ = -\Psi.$$

Substituting the above into (41), the TVD equation may be expressed as

$$\frac{\Delta u_i^{n+1}}{\Delta t} = -sa \frac{1}{\Delta x} (\Delta u_i^{n+1} - \Delta u_{i-1}^{n+1}) + \frac{\Psi \Delta x}{2\Delta x^2} (\Delta u_i^{n+1} - 2\Delta u_{i-1}^{n+1} + \Delta u_{i-2}^{n+1}) - \frac{1}{\Delta x} (f_i^n - f_{i-1}^n) + \frac{\Psi \Delta x}{2\Delta x^2} (f_i^n - 2f_{i-1}^n + f_{i-2}^n). \tag{41b}$$

If we set

$$s_1 = s, \quad s_2 = \frac{s\Delta x \Psi}{a\Delta t}, \quad \Psi = \frac{a\Delta t}{\Delta x}, \quad s_2 = s_1,$$

it is seen that the FDV equation (38) becomes identical to the TVD equation (41b) or *vice versa*. Note that in TVD either a^+ or a^- must be chosen from the flow field and the variation parameters s_1 and s_2 in FDV are automatically calculated. Of course, the precise shock-capturing mechanism of both methods is not exactly the same, because all the assumptions

made above are not true in general. However, it is interesting to note that the first-order convection variation parameter s_1 is related to the TVD limiter function Ψ as

$$s_1 = \frac{s\Delta x}{a\Delta t}\,\Psi, \tag{42}$$

in which it is shown that the convection variation parameters (s_1, s_2) are proportional or equivalent to the TVD limiter functions.

Considering that the motivations and procedures of derivation are completely different, the analogy between the TVD scheme and FDV formulation as demonstrated above is remarkable. Notice that, beyond this analogy, the FDV formulation is to couple the convection variation parameters (s_1, s_2) with all other variation parameters (s_3, s_4, s_5, s_6) so that shock wave interactions with all other physical properties can be resolved. They are involved also in transitions and interactions of compressible/incompressible, inviscid/viscous and laminar/turbulent flows. Although the shock tube problems in Example (2) (Figure 2) was solved using the general program based on (16), the identical results are obtained from the solution based on (37) or (38). This is because all terms not involved in the convection variation parameters are zero in (16) as determined from the flow field of the shock tube.

6. TRANSITIONS AND INTERACTIONS BETWEEN COMPRESSIBLE AND INCOMPRESSIBLE FLOWS

One of the most significant aspects of the FDV scheme is that for low Mach numbers (incompressible flow) the scheme will automatically adjust itself to prevent pressure oscillations. Notice that second derivatives of pressure appear in momentum (26) and continuity (29), acting as numerical diffusion. This adjustment is analogous to the pressure correction scheme (via pressure Poisson equation) for incompressible flows. Otherwise, the FDV scheme is capable of shock wave resolutions at high Mach numbers, and particularly well-suited for dealing with interactions between shock waves and turbulent boundary layers where an aggregation of high and low Mach numbers exist. In this case, the inviscid and viscous interactions are allowed to take place. To this end, the second-order variation parameters play the role of artificial viscosity needed for shock wave resolutions in the presence of flow diffusion due to physical viscosity.

In order to understand how the FDV scheme handles computations involving both compressible and incompressible flows, fundamental definitions of pressure as involved in compressible and incompressible flows must be recognized. Consider in the following that the fluid is a perfect gas and that the total energy is given by

$$E = c_p T - \frac{p}{\rho} + \frac{1}{2} v_i v_i. \tag{43}$$

The momentum equation for steady state incompressible rotational flow may be integrated to give

$$\int \left(p + \frac{1}{2}\rho v_j v_j \right)_{,i} \mathrm{d}x_i = \int (\mu v_{i,jj} + \rho \varepsilon_{ijk} v_j \omega_k)\,\mathrm{d}x_i, \quad p + \frac{1}{2}\rho v_j v_j = p_0 + Q, \tag{44}$$

with

$$Q = \frac{1}{n} \int (\mu v_{i,jj} + \rho \varepsilon_{ijk} v_j \omega_k) \, \mathrm{d}x_i,$$

where p_0 is the constant of integration, and n is the spatial dimension.

Substituting (43) into (44) leads to the following relationship:

$$p_0 = \rho (c_p T + v_i v_i - E) - Q. \tag{45}$$

If p_0 as given by (45) remains a constant, equivalent to a stagnation (total) pressure, then the compressible flow as assumed in the conservation form of the Navier–Stokes system of equations has now been turned into an incompressible flow, which is expected to occur when the flow velocity is sufficiently reduced (approximately $0.1 \leq M < 0.3$ for air). Thus, (45) serves as an equivalent equation of state for an incompressible flow. This can be identified nodal point by nodal point or element by element for the entire domain.

We may begin with the condition given by (44) for compressible flows. If computations are involved in low-speed flows then the governing equations and computational schemes initially intended for high-speed compressible flows are automatically switched to those for low-speed incompressible flows with p_0 remaining constant for all low Mach number flows (approximately $0.1 \leq M < 0.3$) based on the flow field-dependent variation parameters. If the flow reverses to compressible, then the stagnation pressure becomes variable, allowing the density to change. This is clearly demonstrated in Example (3) and Figure 3 for driven cavity problems.

An advantage of the FDV scheme is to avoid the so-called pressure correction process, preconditioning approach, or the implementation of a separate hyperbolic–elliptic equation as is the case with other computational schemes designed to accommodate flows of all speed regimes. In the case of the FDV formulation, a computational scheme similar to pressure correction (keeping pressure from oscillating) automatically arises by means of the Mach number and Reynolds number-dependent variation parameters. This approach is particularly useful for the inviscid–viscous interaction regions and boundary layers close to the wall, such as in hypersonic aircraft or shock wave turbulent boundary layer interactions in general.

7. TRANSITIONS AND INTERACTIONS BETWEEN LAMINAR AND TURBULENT FLOWS

When inviscid flow becomes viscous, we may expect that the flow may become laminar or turbulent through inviscid/viscous interactions across the boundary layer. Below the laminar boundary layer, if viscous actions are significant, then the fluid particles are unstable, causing the changes of Mach number and Reynolds number between adjacent nodal points (assuming they are closely spaced) to be irregular, the phenomenon known as transition instability prior to the state of full turbulence. How can these processes be modelled in FDV formulation?

Fluctuations due to turbulence are characterized by the presence of the terms such as

$$s_3 \Delta \tau_{ij} = \frac{\sqrt{Re_{\max}^2 - Re_{\min}^2}}{Re_{\min}} \Delta \tau_{ij} \tag{46}$$

Physically, the above quantity represents the fluctuations of total stresses (physical viscous stresses plus Reynolds stresses) controlled by the Reynolds number changes between the local adjacent nodal points. Thus, the FDV solution contains the sum of the mean flow variables and the fluctuation parts of the variables.

Once the solution of the Navier–Stokes system of equations is carried out and all flow variables are determined, then we compute fluctuation part, f' of any variable f,

$$f' = f - \bar{f}, \tag{47}$$

where f and $\bar{f}$ denote the Navier–Stokes solution and its time or mass average respectively. This process may be replaced by the fast Fourier transform of the Navier–Stokes solution. Unsteady turbulence statistics (turbulent kinetic energy, Reynolds stresses and various energy spectra) can be calculated once the fluctuation quantities of all variables are determined. See Example (4) and Figure 4 for the supersonic turbulent flow on a compression corner.

Although the solutions of the Navier–Stokes system of equations using FDV are assumed to contain the fluctuation parts as well as the mean quantities, it will be unlikely that such information is reliable when the Reynolds number is very high and if mesh refinements are not adequate to resolve Kolmogorov microscales. In this case, it is necessary to invoke the level of mesh refinements as required for DNS.

It is important to recognize that unsteadiness in turbulent fluctuations may prevail in the vicinity of the wall, although a steady state may have been reached far away from the wall. This situation can easily be verified by noting that $\Delta\mathbf{U}^{n+1}$ will vanish only in the region far away from the wall, but remain fluctuating in the vicinity of the wall, as dictated by the changes of Mach number in the variation parameter s_3 between the nodal points and fluctuations of the stresses due to both physical and turbulent viscosities in $\Delta\tau_{ij}$ characterized by (46).

8. EXAMPLE PROBLEMS

To validate the FDV theory, numerical example problems for various physical phenomena have been solved. Previously, the computer codes for three-dimensional geometries were tested [13,14]. Some selected examples in this paper include: (1) contour plots of calculated variation parameters to test flow field-dependent properties, (2) shock tube problems to test shock-capturing ability, (3) driven cavity flow problems to test incompressibility/compressibility characteristics, and (4) accuracy of FDV simulation for turbulent flows in supersonic flows.

(1) *Contour plots of calculated variation parameters to test flow field-dependent properties*

To explain the role of the variation parameters, we examine the FDV solution for the flow over a ten degree compression corner at $M_\infty = 3$, $Re = 1.68^4$ (Figure 1). Note that the contour distributions of the first-order convection variation parameter s_1 resemble the flow field depicting the shock waves as shown in Figure 1(a). The second-order convection variation parameter s_2, which represents the artificial viscosity for shock-capturing, closely follows s_1 with somewhat wavy distributions ($s_2 = s_1^{1/4}$). It is seen that the $s_1 = 0$ region (no changes in Mach number) is clearly distinguished from the region near the wall where s_1 is close to unity (rapid changes of Mach number). Note that $s_1 = 0$ changes to $s_1 = 1$ abruptly along the line where the shock is expected to appear.

It is seen that the contour distributions of the first-order diffusion variation parameter s_3 resemble the boundary layer formation in the vicinity of the wall with thickening of contours toward the wall as compared with the first-order convection variation parameter s_1. The second-order diffusion variation parameter s_4 whose role is to provide numerical diffusion for stability for the calculation of fluctuations of turbulent motions follows the trend of s_3 with wavy distributions ($s_4 = s_3^{1/4}$). No changes in Reynolds number is indicated by $s_3 = 0$ in the upper upstream region, which coincides with $s_1 = 0$ for convection as expected.

The actual flow field calculations based on these variation parameters are shown in Figure 2(b). As the FDV theory dictates, the first-order variation parameters (s_1, s_3) control the physics and accuracy, whereas the second-order variation parameters (s_2, s_4) address numerical diffusion for stability. These variation parameters are updated throughout the computational process until the steady state is reached, with their contours continuously resembling the actual flow field.

It should be noted that the physical interactions between inviscid/viscous, compressible/incompressible and laminar/turbulent flows are simultaneously controlled by the first- and second-order convection/diffusion variation parameters. These assessments will be verified from additional example problems presented below.

(2) ***Shock tube problems to test shock-capturing ability***

Two shock tube problems of differing shock strengths of the following data (SI unit) are tested:

(a) $p_L = 10^5$, $\rho_L = 1$, $p_R = 10^4$, $\rho_R = 0.125$,
(b) $p_L = 10^5$, $\rho_L = 1$, $p_R = 10^3$, $\rho_R = 0.01$.

The FDV solutions for the above shock tube cases ($u_L = u_R = 0$) indicate perfect agreements with the analytical solutions as shown in Figure 2. It is believed that the shock-capturing

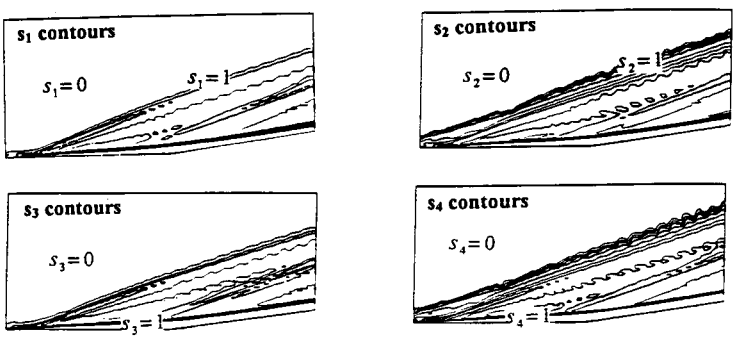

(a) Calculated variation parameter contour distributions

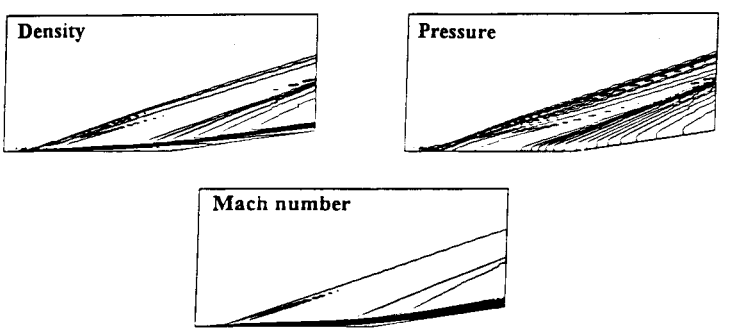

(b) Flowfield contour distributions

Figure 1. Contour plots of calculated variation parameters to test flow field-dependent properties. Note that variation parameter contours resemble those of flow fields themselves.

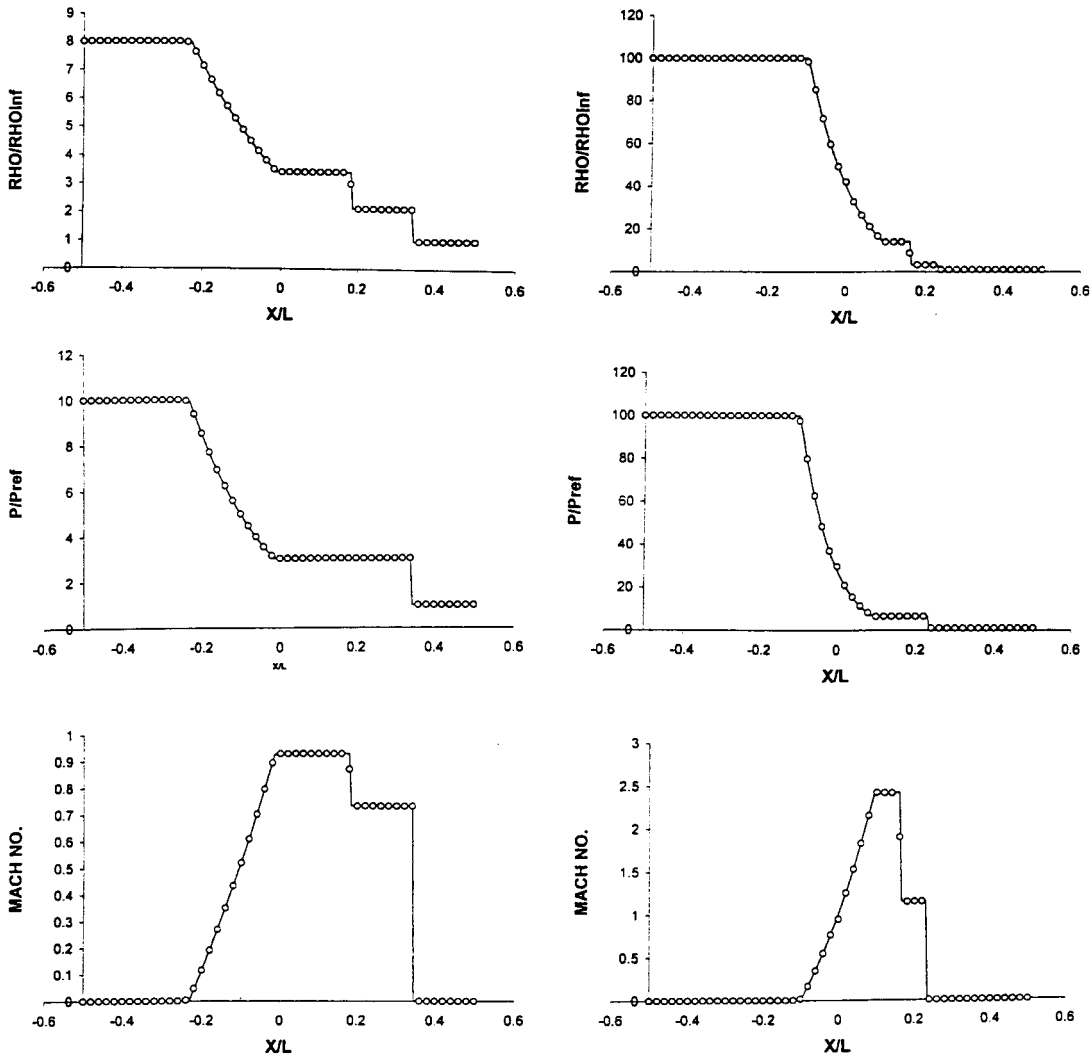

Figure 2. Shock tube problems to test shock capturing ability. ○, FDV; —, analytical.

capability of FDV scheme is superior. To appreciate this point, let us re-examine Equations (22), (25) and (28). Notice that there are convection terms with the non-fluctuation quantities without variation parameters which merely represent the standard artificial viscosity for non-fluctuation terms. In addition, there are other convective terms with the fluctuation quantities associated with the variation parameter s_1 and the extra terms with s_2. Here, the s_2 terms represent the stabilization of the fluctuation parts of the convection variables (pressure and velocity). If the variation parameters are replaced by the definitions given in (8)–(14), then such a scheme is seen to play a role of the high resolution shock-capturing, much more

sophisticated than other numerical schemes, such as TVD limiters with the FDV equivalence given by (37). This is because the shock-capturing scheme is not only involved in Mach number changes between adjacent nodal points, but also coupled with all other variation parameters, contributing to the transitions and interactions of all physical phenomena, such as inviscid/viscous, compressible/incompressible and laminar/turbulent flows.

(3) ***Driven cavity flow problems to test compressibility/incompressibility characteristics***

This example demonstrates that the FDV scheme is capable of reaching the incompressible limit at low speeds as well as the shock-capturing capability at high speeds. The cavity flow problem [14] is examined here for two different Mach numbers ($M = 0.01$ and 0.1). Density distributions (Figure 3(a)) for $M = 0.01$ are constant throughout the domain, whereas at $M = 0.1$ we note that variations begin to occur near the downstream upper region. The most significant feature is the distribution of the stagnation (total) pressure (Figure 3(b)) as calculated from Equation (45), indicating that the stagnation pressure is constant at $M = 0.01$ and it begins to vary at $M = 0.1$, almost exactly the same way as density. This proves that Equation (45) acts as the equation of state encompassing the incompressible and compressible flows. Comparisons of the FDV solutions for the velocity distributions at the centerlines (Figure 3(c)) confirm the trend disclosed in Figure 3(a) and (b). The velocity distributions for $M = 0.01$ are identical to the results of the experimental data for incompressible flow, whereas the solution for $M = 0.1$ (compressible effect present) deviates from the incompressible case. The evidence is overwhelming that the FDV scheme is capable of treating the transition automatically between the incompressible and compressible limit.

(4) ***Accuracy of FDV simulation for turbulent flows in supersonic compression corner***

Does the FDV theory simulate turbulence? This remains a central issue and demands a rigorous search for many years to come. However, a simple example presented here indicates that the response is affirmative. Let us consider a compression corner flow ($M_\infty = 2.25$, $Re = 10^5$) considered in [14]. The FDV solution is carried out to the steady state. Expecting that the steady state mean flow variables contain the fluctuation parts which are unsteady, we perform time averages of approximately ten time steps at a time. Taking a difference between the FDV solution and the time averages, we calculate the fluctuation parts (Equation (47)). Representative results for the horizontal and vertical fluctuation velocity components at two vertical locations (close to the wall, $y = 0.001$ m; away from the wall, $y = 0.004$ m) along the compression corner are shown Figure 4(a). Clearly, the unsteadiness of turbulent fluctuations is evident near the wall, whereas this trend is subdued greatly away from the wall. The Reynolds stresses are calculated from these fluctuation velocity components as shown in Figure 4(b). Note that the high Reynolds stresses are concentrated in the regions of boundary layers. These fluctuation velocity components and Reynolds stresses contribute to the turbulent kinetic energy as shown in Figure 4(c). A mild peak occurs close to the wall upstream of the compression corner, whereas the turbulent kinetic energy increases drastically some distance away from the wall downstream of the compression corner. Finally, the FDV solution is compared with the experimental data and the k–ε model in Figure 4(d). Agreements of the FDV solution with the experimental data are remarkable. As the Mach number increases, however, mesh refinements will be required to maintain the accuracy of the FDV solution. Kolmogorov turbulence microscales can not be resolved unless DNS mesh refinements are provided.

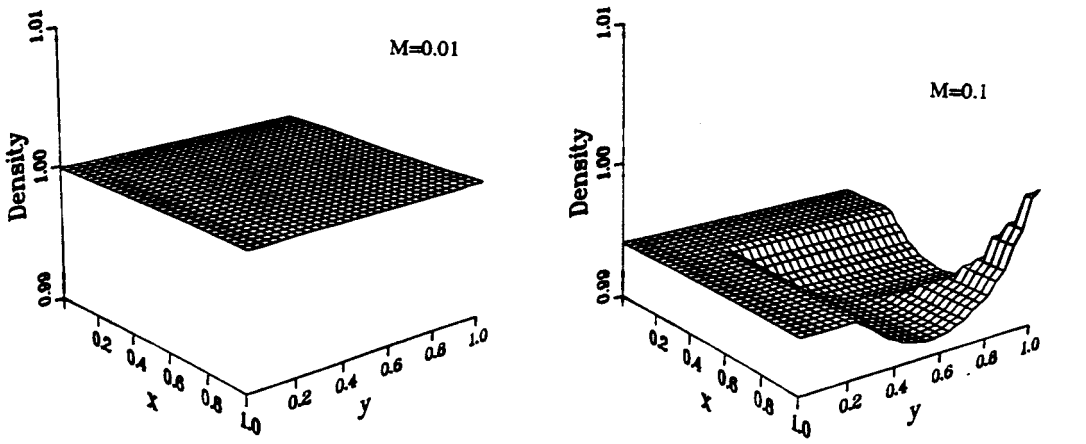

(a) Density distributions

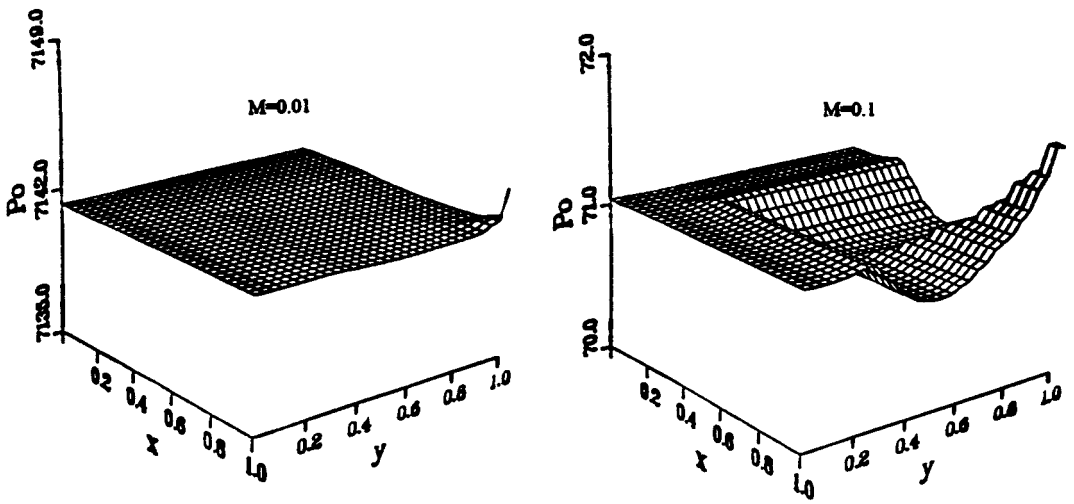

(b) Stagnation (total) pressure distributions

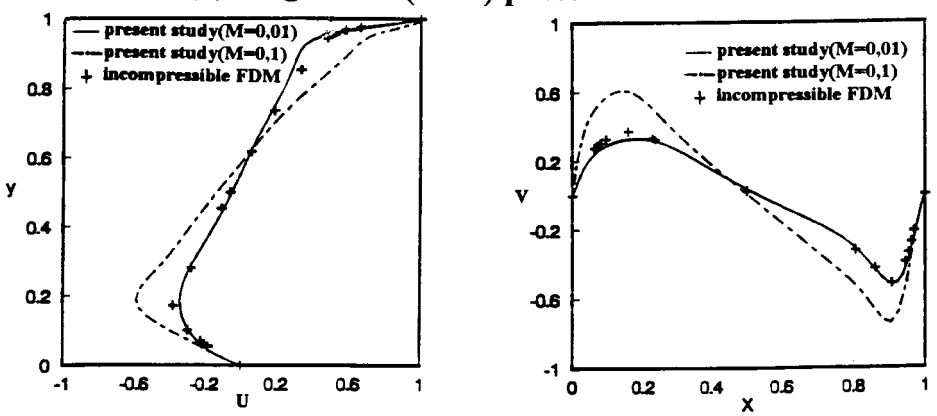

(c) Comparison of velocity distributions with experiments

Figure 3. Driven cavity flow problems to test incompressibility/compressibility characteristics.

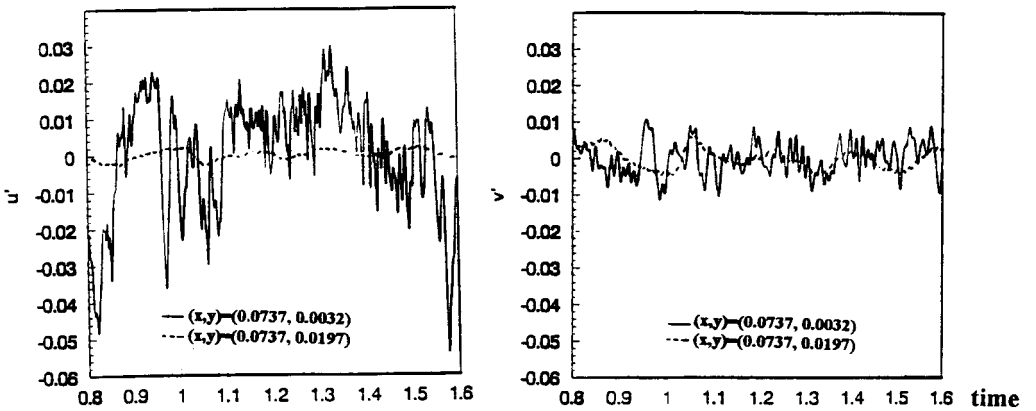

(a) Fluctuation velocity components

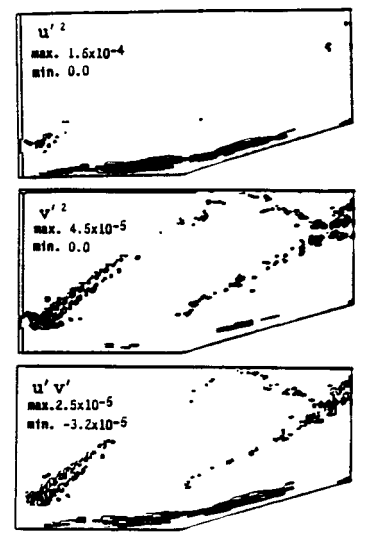

(b) Reynolds stress distributions

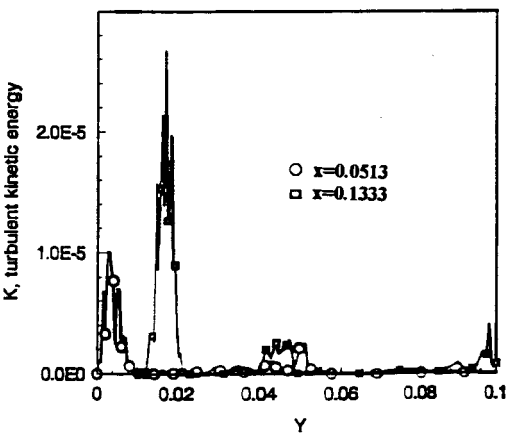

(c) Turbulent kinetic energy

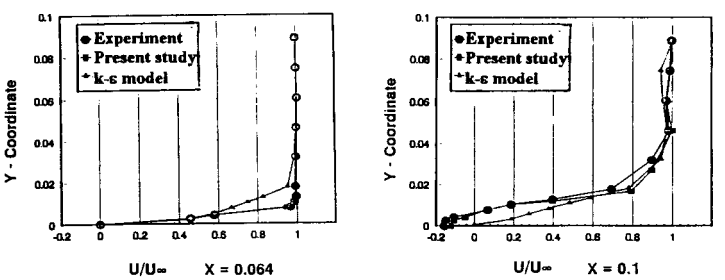

(d) Comparion of FDV mean flow solution vs experiments and $k-\varepsilon$ model

Figure 4. Accuracy of FDV simulation for turbulent flows in supersonic flows ($M = 2.25$, $Re = 10^5$).

9. CONCLUSIONS

Transitions and interactions between inviscid/viscous, compressible/incompressible and laminar/turbulent flows can be resolved by the FDV theory. It is shown that variation parameters initially introduced in the Taylor series expansion of the conservation variables of the Navier–Stokes system of equations are translated into flow field-dependent physical parameters responsible for the characterization of fluid flows. In particular, the convection variation parameters (s_1, s_2) are identified as equivalent to the TVD limiter functions. The FDV equations are shown to contain the terms of fluctuation variables automatically generated in due course of developments, varying in time and space, but following the current physical phenomena. In addition, adequate numerical controls (artificial viscosity) to address both non-fluctuating and fluctuating parts of variables are automatically activated according to the current flow field. It has been shown that practically all existing numerical schemes in FDM and FEM are the special cases of the FDV theory.

Some simple example problems have demonstrated most of the features available in the FDV theory. It was shown that the calculated variation parameters resemble the flow field itself. Shock tube problems proved excellent shock-capturing capabilities. The program capable of solving supersonic flows is used to resolve incompressible flows of driven cavity problems, with the transition from incompressibility to compressibility clearly recognized. Finally, the supersonic compressible turbulent viscous flow on a compression corner was solved, indicating that the FDV simulation does contain turbulent fluctuations and that the turbulent mean flow is accurately resolved.

One of the most significant tasks to be completed in the near future is the three-dimensional simulation of the triple shock wave turbulent boundary layer interactions, followed by reacting flows and combustion. The role of variation parameters due to various definitions of Damkohler numbers should be examined to determine how they contribute to resolving convergence in stiff equations for combustion problems. New and additional features of the FDV theory may be revealed as more example problems are solved.

ACKNOWLEDGMENTS

The work presented in this paper is based on the research supported by AFOSR with Len Sakell as technical monitor. The author would like to thank the many graduate students who programmed the theory and produced many numerical examples. Among them are K.T. Yoon, G.W. Heard, S.A. Garcia, S.Y. Moon and R.G. Schunk.

REFERENCES

1. Y.H. Choi and C.L. Merkle, 'The application of preconditioning to viscous flows', *J. Comput. Phys.*, **105**, 207–223 (1993).
2. C.L. Merkle, J.Y. Sullivan, P.E.O. Buelow and S. Venkateswaran, 'Computation of flows with arbitrary equations of state', *AIAA J.*, **36**, 515–531 (1998).
3. G.S. Settles and D.S. Dolling, 'Swept shock/boundary layer interactions—tutorial and update', *AIAA Paper*, *90-0375*, January 1990.
4. T.J. Garrison, G.S. Settles and C.C. Hortsman, 'Measurements of the triple shock wave/turbulent boundary layer interactions', *AIAA J.*, **34**, 57–64 (1996).
5. D. Gaitonde and J.S. Shang, 'Shock pattern of a triple shock turbulent interaction', *AIAA J.*, **36**, 113–115 (1998).
6. A. Harten, 'High resolution schemes for hyperbolic conservation laws', *J. Comput. Phys.*, **49**, 151–164 (1983).
7. A. Harten, 'On a class of high resolution total variation stable finite difference schemes', *SIAM J. Numer. Anal.*, **21**, 1–23 (1984).

8. P.L. Roe, 'Generalized formulation of TVD Lax–Wendroff schemes', *ICASE Report 84-53*, *NASA CR-172478*, 1984.
9. P.K Sweby, 'High resolution schemes using flux limiters for hyperbolic conservation laws', *SIAM J. Numer. Anal.*, **21**, 995–1011 (1984).
10. B. van Leer, 'Towards the ultimate conservative difference scheme. II. Monotonicity and conservation combined in a second-order scheme', *J. Comput. Phys.*, **14**, 361–370 (1974).
11. R.M. Warming and R.F. Warming, 'An implicit factored scheme for the compressible Navier–Stokes equations', *AIAA J.*, **16**, 393–401 (1978).
12. D.D. Knight, T. Garrison., G.S. Settles, A.A. Zheltovodov, A.I. Maksimoov, A.M. Shevchenko and S.S. Vorontsov, 'Asymmetric crossing-shock wave/turbulent boundary layer interactions', *AIAA J.*, **33**, 2241–2249 (1995).
13. K.T. Yoon and T.J. Chung, 'Three-dimensional mixed explicit–implicit generalized Galerkin spectral element methods for high-speed turbulent compressible flows', *Comput. Methods Appl. Mech. Eng.*, **135**, 343–367 (1996).
14. K.T. Yoon, S.Y. Moon, G.A Garcia, G.W. Heard and T.J. Chung, 'Flow field-dependent mixed explicit–implicit (FDMEI) methods for high and low speed and compressible and incompressible flows', *Comput. Methods Appl. Mech. Eng.*, **151**, 75–104 (1998).
15. S. Sarkar, 'Application of Reynolds stress turbulent mode to the compressible shear layer', *AIAA Paper*, *90-1465*, 1990.
16. O. Zeman, 'Dilatation dissipation: the concept and application in modeling compressible mixing layers', *Phys. Fluids A*, **2**, 178–188 (1990).
17. G. Hauke and T.J.R. Hughes, 'A comparative study of different sets of variables for solving compressible and incompressible flows', *Comput. Methods Appl. Mech. Eng.*, **153**, 1–44 (1998).
18. O.C. Ziekiewicz and R. Codina, 'A general algorithm for compressible and incompressible flow, Part I. The split, characteristic-based scheme', *Comput. Methods Appl. Mech. Eng.*, **20**, 869–885 (1998).
19. C.E. Beaumann and J.T. Oden, 'A discontinuous hp finite element methods for the solution of the Navier–Stokes equations', *10th Int. Symp. Finite Elements in Fluids*, University of Arizona, January 12–14, 1998.
20. T.J. Chung, *Computational Fluid Dynamics*, Cambridge University Press, Cambridge, to be published.
21. R. Codina, 'Comparison of some finite element methods for solving the diffusion–convection–reaction equation', *Comput. Methods Appl. Mech. Eng.*, **156**, 185–210 (1998).

